Increased risk of a shutdown of ocean convection posed by warm North Atlantic summers

Marilena Oltmanns*

moltmanns@geomar.de

Johannes Karstensen

jkarstensen@geomar.de

Jürgen Fischer

jfischer@geomar.de

GEOMAR Helmholtz Centre for Ocean Research Kiel

*Corresponding author

A shutdown of ocean convection in the subpolar North Atlantic, triggered by enhanced melting over Greenland, is regarded as a potential transition point into a fundamentally different climate regime[1,2,3]. Noting that a key uncertainty for future convection resides in the relative importance of melting in summer and the atmospheric forcing in winter, we investigate the extent to which summer conditions constrain convection with a comprehensive data set, including over a decade long hydrographic records from the convection regions. We find that warm and fresh summers, characterized by increased sea surface temperatures, freshwater concentrations and melting, are accompanied by reduced heat and buoyancy losses in winter, which entail a longer persistence of the freshwater near the surface and contribute to delaying convection. By shortening the time span for the convective freshwater export, the identified seasonal dynamics introduce a potentially critical threshold, that is crossed when substantial amounts of freshwater from one summer are carried over into the next and accumulate. Warm and fresh summers in the Irminger Sea are followed by particularly short convection periods, and we estimate that in the winter 2010–2011, after the warmest and freshest Irminger Sea summer on our record, $\sim$40% of the surface freshwater were retained.

Each summer, the subpolar gyre (Figure 1a) warms and freshens, and each winter, intense air-sea fluxes cause the surface water to lose buoyancy and mix the freshwater into the interior ocean (Supplementary Figures 1 and 2). The downward mixing represents an integral component of the large-scale Atlantic overturning circulation[4] which advects heat northward and thus contributes to the relatively mild North Atlantic climate[5]. Yet, with regard to the rising meltwater fluxes from Greenland[6], there is a growing chance that the heat losses in winter are not able to overcome the resulting vertical salinity gradient with potentially far-reaching climatic consequences.

One winter, in which surface freshwater had a clear impact on convection, occurred in 2010–2011 when a layer of colder, fresher water was situated above warmer, saltier water (Figure 1b). To diagnose causes for the reduced surface salinity, we examine the hydrographic conditions in the preceding summer. Mooring observations from the Irminger Sea reveal a warm and fresh surface layer (Figure 2a and b), and remote sensing data depict increased sea surface temperatures (SST), covering a broad area around the mooring and near the southeast Greenland shelf, where meltwater is expected[7] (Figure 2c). Considering that neither cold and fresh Polar Water nor warm and salty Atlantic Water matches the hydrographic properties of the surface water in these regions — being warm and fresh — we speculate that it has a continental origin and was modified by surface heating.

To investigate how influential these summer conditions generally are for convection, we start by characterizing fresh summers. After identifying them based on negative sea surface salinity (SSS) anomalies in the Irminger[8,9] and Labrador Sea[10,11] convection regions, we find that fresh summers in the Irminger Sea are accompanied by increased SST over the subpolar gyre (Figure 2d) and a positive sea level pressure (SLP) anomaly over the Irminger Sea (not shown). Fresh summers in the Labrador Sea, by comparison, preferentially occur when the summertime index of the North Atlantic Oscillation is negative ($r = 0.64$), which indicates raised air pressure and temperatures over Greenland[12] and has previously been connected with enhanced surface melt[13]. Noting that at both convection sites, negative SSS anomalies correlate with overall warmer conditions and melting ($r = 0.67$ for the Irminger Sea and $r = 0.65$ for the Labrador Sea, Supplementary Figure 3), we hypothesize that they are related, although differences in the amplitude and location of the atmospheric circulation patterns may lead to changes in the detailed freshwater distribution. All specified correlations are significant at the 95% confidence level, assessed by means of a two-sided t-test.

Having established that fresh summers are associated with increased SST or negative NAO phases — both of which have been recorded for a much longer time span than SSS — we utilize these dependencies to investigate the ensuing hydrographic and atmospheric evolution in fall and winter. To describe fresh summers in the Irminger Sea, we construct an index based on SST in the Irminger Sea during August (F_{IS}, Supplementary Figure 3a) while fresh summers in the Labrador Sea are specified by the negative NAO index from July through August (F_{LS}, Supplementary Figure 3b). This also has the advantage that both indices take account of a wider area instead of a single location.

In situ observations from the Labrador Sea reveal that the hydrographic evolution in fall and winter is significantly constrained by the summer conditions. After warm and fresh summers, defined by either index, the ocean surface remains anomalously fresh, with more saline water beneath (Figure 3a and b). The corresponding temperature correlations match those for salinity at depth, but show a weaker dependence near the surface, with higher SST after fresh Irminger Sea summers (Figure 3c and d). As a result, the net density gradient is increased over the upper ∼300 m in mid winter, with the correlation being larger after fresh Irminger Sea summers (Figure 3e and f).

In the Irminger Sea, the surface salinity in winter is likewise anti-correlated with F_{IS}, but not significantly connected with F_{LS}, while the salinity and temperature correlations below the surface are similar to those in the Labrador Sea (Supplementary Figure 4a–d). Consequently, stratification correlates with F_{IS}, but not with F_{LS} (Supplementary Figure 4e and f). As the stratification in both basins exhibits higher correlations with F_{IS} than with F_{LS}, we infer that fresh Irminger Sea summers are more influential for winter convection than fresh Labrador Sea summers. In addition, we find that stratification in the Labrador Sea, often regarded as the primary convective region[14], is more sensitive to the summer conditions than stratification in the Irminger Sea.

To quantify the relative contributions of the salinity and temperature gradients to the increased stratification, we use the linearized equation of state and calculate the heat losses needed to offset these gradients down to 200 m depth. This level corresponds to the approximate upper edge of the seasonal subsurface salinity maximum (Supplementary Figure 2c) and we do not expect the freshwater to have an appreciable impact on convection, once it is mixed beneath. Regressing the results on both summer indices, we find that the salinity anomaly accounts for an energy surplus of $\sim 2.8 \cdot 10^8$ J m^{-2} after fresh Irminger Sea summers and $\sim 4.8 \cdot 10^8$ J m^{-2} after fresh Labrador Sea summers (Supplementary Figure 5a and b). Since the temperature anomaly originating from fresh Labrador Sea summers partially compensates for the enhanced surface freshening, the net density gradient is significantly increased only after fresh Irminger Sea summers, requiring an additional heat loss of $\sim 2.4 \cdot 10^8$ J m^{-2} to be eroded (Supplementary Figure 5c and d).

Noting that the stratification anomaly intensifies in winter (Supplementary Figure 5c), we infer that it may be reinforced by a positive feedback. Thus, we next investigate the extent to which the atmospheric forcing is constrained by the summer conditions. Reanalysis data show that fresh Irminger Sea summers are followed by reduced SLP over the subpolar region in September and October, driving larger ocean heat losses (Figure 4a and b). The subsequent atmospheric circulation from November through March is characterized by a positive

SLP anomaly over Greenland and the surrounding ocean and the heat losses are suppressed, especially in the Labrador Sea (Figure 4c and 4d).

Integrating the heat flux anomalies (positive downward) from September through March, we find that their net effect is positive (Supplementary Figure 6a) with an added heat gain of $\sim 2.6 \cdot 10^8$ J m^{-2}, corresponding to $\sim$9% of the climatological average. The net buoyancy flux anomalies, which include the combined effects of the surface heat and freshwater fluxes[15], are comparable to those of the heat fluxes (Supplementary Figure 6b), with the impact of the freshwater fluxes being negligible compared to that of the heat fluxes. Employing F_{LS} instead of F_{IS} yields qualitatively similar distributions of the heat and buoyancy flux anomalies, but with reduced amplitudes (Supplementary Figure 6c and d).

The negative SLP anomaly in early fall (Figure 4a) resembles the transient atmospheric response to positive SST anomalies that has previously been characterized in model studies[16,17]. Being maintained by the increased SST, it typically lasts a few weeks before it transforms into the equilibrium response[16,17], which conforms to the negative NAO mode (Figure 4c)[18,19,20]. As the development of both responses has been explained by the SST anomaly, we attribute the high predictability of the atmosphere to the summer conditions, acknowledging that anomalously warm subsurface water, entrained into the mixed layer in fall and winter, can extend the response[21]. This inference is consistent with the larger atmospheric and hydrographic correlations with F_{IS} compared to F_{LS} because only after fresh Irminger Sea summers is the SST anomaly strong enough to survive the enhanced heat losses in fall (Supplementary Figure 4c and d).

After ascertaining the relevance of the summer conditions and the subsequent atmospheric evolution for convection, we next examine their longer-term variability (Supplementary Figure 7a). Despite substantial interannual variations, we detect significant trends in the SST and both atmospheric responses over the period 1990–2014. The SST in the Irminger Sea has increased by more than 1.5 °C throughout the year but most in summer (Figure 5a and b), the SLP has significantly decreased in fall (not shown), and the change in the heat fluxes peaks over the Labrador Sea during winter (Figure 5c and d).

While these trends do not imply any continuation of the summer warming and its responses into the future, in particular with regard to deep ocean convection in the years 2013–2016[22,23,24], their seasonality suggests that the identified seasonal dependencies also hold on decadal time scales. On even longer time scales, the robustness of the results is investigated with SST data from the Hadley Centre and the Greenland Blocking Index (GBI)[25]. The GBI is a measure of the surface pressure over Greenland and thus, closely related to the equilibrium atmospheric response after warm summers (Figure 4c). Noting that it favorably correlates with the winter heat fluxes over the Labrador Sea ($r =$ 0.92, based on 25 winters), we use it to describe their variability from 1950 to 2014.

A coherence analysis of the GBI and the summer SST shows that the atmospheric correlations are largest on decadal and longer time scales (Supplementary Figure 7b and c), which we attribute to reemerging deep water, formed in previous years, that reinforces the equilibrium response in winter[21]. Considering that the hydrographic correlations were based on interannual time scales, our results suggest that fresh Irminger Sea summers within extended warm periods provide conditions particularly conducive to a stable stratification because then, the oceanic and atmospheric drivers combine.

Among the implications of a more stable stratification is a delayed onset and overall shorter duration of convection (Supplementary Figure 8), which in turn, implies less time for the convective export of surface freshwater. With regard to the pronounced seasonal cycle in the subpolar hydrography (Supplementary Figure 2), limiting the annual freshwater removal can lead to a nonlinear response in the freshwater abundance and thus, the crossing of a critical threshold, when substantial amounts of freshwater from two or more summers accumulate and prevent convection. Although eddies can export freshwater[26] or import salt[27] horizontally, and exceptionally strong heat losses may potentially erode a surface layer with the cumulative freshwater from two summers, it is unclear how efficient these mechanisms are in comparison to the expected rising meltwater fluxes[6,28].

To place our results in this context, we estimate how much surface freshwater was retained through each of the investigated winters. Since it is the salinity gradient (not the absolute salinity) that controls the magnitude of the mixing, we first identify the maximum salinity at 200 m depth after each summer as background salinity S_{ref} with which we contrast the surface values. Integrating the freshwater anomaly $\frac{S_{ref}-S}{S_{ref}}$ over the upper 200 m, we then determine the amount carried over into the next season (see Supplementary Figure 9 for an example). Thus, we find that the freshwater transfer, expressed either by means of the minimum anomaly or as percentage relative to the assumed maximum, is significantly correlated with both summer indices (Supplementary Table 1). In the winter 2010–2011, in particular, following the warmest Irminger Sea summer on our record, ∼40% of the freshwater were retained (Supplementary Figure 9c).

We conclude that warm and fresh summers in the subpolar North Atlantic are accompanied by reduced heat and buoyancy losses in winter, which entail a longer persistence of the surface freshwater and thus contribute to delaying convection. By shortening the time span for the convective freshwater removal, the identified seasonal relationships introduce a potentially critical threshold on convective stability, that is crossed when substantial amounts of freshwater from two or more summers combine. Warm and fresh summers in the Irminger Sea pose a particularly high risk to convection, and hydrographic observations from the Labrador Sea in 2010–2011, following the warmest and freshest Irminger Sea summer on our record, indicate that ∼40% of the surface freshwater were retained throughout winter.

References

[1] P. U. Clark et al. “The role of the thermohaline circulation in abrupt climate change”. In: *Nature* 415.6874 (2002), pp. 863–869.

[2] S. Rahmstorf. “Ocean circulation and climate during the past 120,000 years”. In: *Nature* 419.6903 (2002), pp. 207–214.

[3] T. M. Lenton et al. “Tipping elements in the Earth’s climate system”. In: *Proceedings of the national Academy of Sciences* 105.6 (2008), pp. 1786–1793.

[4] M. S. Lozier. “Overturning in the North Atlantic”. In: *Annual review of marine science* 4 (2012), pp. 291–315.

[5] K. E. Trenberth and J. M. Caron. “Estimates of meridional atmosphere and ocean heat transports”. In: *Journal of Climate* 14.16 (2001), pp. 3433–3443.

[6] J. Bamber et al. “Recent large increases in freshwater fluxes from Greenland into the North Atlantic”. In: *Geophysical Research Letters* 39.19 (2012).

[7] SH Mernild et al. “Freshwater flux to Sermilik Fjord, SE Greenland”. In: *The Cryosphere* 4.4 (2010), p. 453.

[8] R. S. Pickart, F. Straneo, and G. W. K. Moore. “Is Labrador Sea water formed in the Irminger basin?” In: *Deep Sea Research Part I: Oceanographic Research Papers* 50.1 (2003), pp. 23–52.

[9] K. Våge et al. “The Irminger Gyre: Circulation, convection, and interannual variability”. In: *Deep Sea Research Part I: Oceanographic Research Papers* 58.5 (2011), pp. 590–614.

[10] K. L. Lavender, R. E. Davis, and W. B. Owens. “Observations of open-ocean deep convection in the Labrador Sea from subsurface floats”. In: *Journal of Physical Oceanography* 32.2 (2002), pp. 511–526.

[11] Robert S Pickart, Daniel J Torres, and R Allyn Clarke. “Hydrography of the Labrador Sea during active convection”. In: *Journal of Physical Oceanography* 32.2 (2002), pp. 428–457.

[12] J. W. Hurrell et al. *An overview of the North Atlantic oscillation*. Wiley Online Library, 2003.

[13] E. Hanna et al. “Atmospheric and oceanic climate forcing of the exceptional Greenland ice sheet surface melt in summer 2012”. In: *International Journal of Climatology* 34.4 (2014), pp. 1022–1037.

[14] John Lazier et al. “Convection and restratification in the Labrador Sea, 1990–2000”. In: *Deep Sea Research Part I: Oceanographic Research Papers* 49.10 (2002), pp. 1819–1835.

[15] Adrian E Gill. *Atmosphere—ocean dynamics*. Elsevier, 2016.

[16] D. Ferreira and C. Frankignoul. “The transient atmospheric response to midlatitude SST anomalies”. In: *Journal of climate* 18.7 (2005), pp. 1049–1067.

[17] C. Deser, R. A. Tomas, and S. Peng. “The transient atmospheric circulation response to North Atlantic SST and sea ice anomalies”. In: *Journal of Climate* 20.18 (2007), pp. 4751–4767.

[18] A. Czaja and C. Frankignoul. “Observed impact of Atlantic SST anomalies on the North Atlantic Oscillation”. In: *Journal of Climate* 15.6 (2002), pp. 606–623.

[19] G. Gastineau, F. D’Andrea, and C. Frankignoul. “Atmospheric response to the North Atlantic Ocean variability on seasonal to decadal time scales”. In: *Climate dynamics* 40.9-10 (2013), pp. 2311–2330.

[20] G. Gastineau et al. “Mechanisms Determining the Winter Atmospheric Response to the Atlantic Overturning Circulation”. In: *Journal of Climate* 29.10 (2016), pp. 3767–3785.

[21] C. Cassou, C. Deser, and M. A. Alexander. "Investigating the impact of reemerging sea surface temperature anomalies on the winter atmospheric circulation over the North Atlantic". In: *Journal of climate* 20.14 (2007), pp. 3510–3526.

[22] F Fröb et al. "Irminger Sea deep convection injects oxygen and anthropogenic carbon to the ocean interior". In: *Nature communications* 7 (2016).

[23] M. F. de Jong and L. de Steur. "Strong winter cooling over the Irminger Sea in winter 2014–2015, exceptional deep convection, and the emergence of anomalously low SST". In: *Geophysical Research Letters* 43.13 (2016), pp. 7106–7113.

[24] I. Yashayaev and J. W. Loder. "Further intensification of deep convection in the Labrador Sea in 2016". In: *Geophysical Research Letters* 44.3 (2017), pp. 1429–1438.

[25] E. Hanna et al. "Greenland Blocking Index 1851–2015: a regional climate change signal". In: *International Journal of Climatology* 36.15 (2016), pp. 4847–4861.

[26] F. Straneo. "Heat and freshwater transport through the central Labrador Sea". In: *Journal of Physical Oceanography* 36.4 (2006), pp. 606–628.

[27] Xue Fan et al. "Observations of Irminger Sea anticyclonic eddies". In: *Journal of Physical Oceanography* 43.4 (2013), pp. 805–823.

[28] T. Stocker. *Climate change 2013: the physical science basis: Working Group I contribution to the Fifth assessment report of the Intergovernmental Panel on Climate Change.* Cambridge University Press, 2014.

Additional information

Correspondence and requests for materials should be addressed to M.O.

Acknowledgments

We thank the staff from NOAA/OAR/ESRL, NCAR and the Hadley Centre for providing the SST data, and from Ssalto/Duacs, AVISO and Cnes for producing and distributing the altimeter products. We also appreciate the efforts that went into the development and management of the Ocean Observatories Initiative. The research in this study contributes to the projects 'Blue-Action' and 'AtlantOS' and was funded by the EU Horizon 2020 Programme under the grant agreements 727852 and 633211. It was further supported by the German Federal Ministry of Education and Research as part of the project 'RACE – Regional Atlantic Circulation and Global Change'.

Author contributions

J.F. and J.K. were involved in the planning, acquisition and processing of the mooring data. M.O. and J.K. conceived the story. M.O. carried out the data analysis and interpreted the results. All authors contributed to writing up the paper.

Competing financial interests statement

The authors declare no competing financial interests.

Method

The hydrographic variability is investigated by means of 13-year-long time series with a 2-week temporal resolution (Supplementary Figure 1), which include the analysis of moored observations in the convection centers, 2990 Argo float profiles in the Labrador Sea and 2614 profiles in the Irminger Sea (Figure 1a). Upon testing different methods for constructing the time series, we found that the best agreement between the mooring and Argo float observations in the Labrador Sea was achieved by averaging the float profiles in each time window after outliers outside one standard deviation around the sample mean (e.g. due to eddies or excursions of the coastal boundary current) were removed. Thus, we took this approach to create the final time series, treating the mooring data like an additional Argo profile, and applied a six-week running mean for increased robustness.

In the Irminger Sea, the best agreement between the float and mooring data was obtained by averaging only the profiles that recorded surface salinities lower than the sample mean in the respective time window because the mooring is located in the fresher part of the region. However, given the good temporal coverage of the mooring observations including at the surface, we based the analyses on the mooring record and only filled the remaining gaps with Argo data. Thus, the results do not change appreciably when different techniques for the float sampling are employed. To identify fresh summers in the Irminger Sea, we avoided any influence of spatial freshwater variability by using only the mooring record.

Other data sets involved in this study are high-resolution remote sensing observations of SST from the AMSR-E satellite for the period 2002–2011, provided by the National Center for Atmospheric Research[29], as well as SST data from the National Oceanic and Atmospheric Administration (NOAA)[30] from 1990 through 2016. We further used the 20th century SST data base from the Hadley Centre[31] for the period 1950–2016, altimetry-based absolute dynamic topography from Aviso[32], SLP and surface fluxes from the ERA-Interim reanalysis[33], distributed by the European Centre for Medium-Range Weather Forecasts, and a satellite-derived melt product that quantifies the surface melt extent over Greenland for the period 1979–2012[34]. To estimate interannual variations in the mean summer melting we averaged the melt extent from July through August. The daily NAO index and the monthly GBI were obtained from NOAA.

Since surface fluxes over the ocean from reanalysis models are often poorly constrained, we validated the net heat and freshwater fluxes from ERA-Interim over the Irminger Sea for the period from August 17, 2015 to January 24, 2016 with direct observations obtained from surface buoys of Ocean Observatories Initiative moorings (`http://oceanobservatories.org/array/global-irminger-sea/`). We found an excellent agreement between these two data sets, with root mean square errors that lie within the uncertainty range of the observations and correlations above 0.8 for the freshwater fluxes and above 0.95 for the heat fluxes (based on a daily time series, totaling 161 independent observations). Considering that these mooring observations are not assimilated by the reanalysis, the good agreement renders credibility to the heat, freshwater and buoyancy fluxes, derived from ERA-Interim, and thus supports the results of this study.

Data availability: The official mooring names are CIS (in the Irminger Sea) and K1 (in the Labrador Sea) and their data is partially deposited in the OceanSITES repository (`http://dods.ndbc.noaa.gov/thredds/catalog/oceansites/DATA/`). The remaining data is available from the corresponding author upon reasonable request.

References

[29] C. L. Gentemann, T. Meissner, and F. J. Wentz. "Accuracy of satellite sea surface temperatures at 7 and 11 GHz". In: *IEEE Transactions on Geoscience and Remote Sensing* 48.3 (2010), pp. 1009–1018.

[30] R. W. Reynolds et al. "Daily high-resolution-blended analyses for sea surface temperature". In: *Journal of Climate* 20.22 (2007), pp. 5473–5496.

[31] N. A. Rayner et al. "Global analyses of sea surface temperature, sea ice, and night marine air temperature since the late nineteenth century". In: *Journal of Geophysical Research: Atmospheres* 108.D14 (2003).

[32] P. Y. Le Traon, F. Nadal, and N. Ducet. "An improved mapping method of multisatellite altimeter data". In: *Journal of atmospheric and oceanic technology* 15.2 (1998), pp. 522–534.

[33] D. P. Dee et al. "The ERA-Interim reanalysis: Configuration and performance of the data assimilation system". In: *Quarterly Journal of the royal meteorological society* 137.656 (2011), pp. 553–597.

[34] T. L. Mote. "Greenland surface melt trends 1973–2007: Evidence of a large increase in 2007". In: *Geophysical Research Letters* 34.22 (2007).

Figure captions

Figure 1 | Labrador Sea, 2010–2011. a, Mean absolute dynamic topography in the subpolar region, with negative values implying a cyclonic circulation. The white contours delineate the regions used for the float sampling, 'LS' and 'IS' refer to the Labrador and Irminger Seas and the circles mark the mooring locations. **b,** Evolution of absolute salinity and potential temperature in the Labrador Sea from November 2010 through August 2011, with contours indicating fresher and colder upper water, obtained from the hydrographic records shown in Supplementary Figure 1.

Figure 2 | Fresh summers in the Irminger Sea. a,b, Mooring observations of a warm, fresh surface layer in the Irminger Sea (location shown in **c**). **c,** 7-day low-pass filtered SST anomalies in summer 2010 from AMSR-E satellite data, where the anomaly is with respect to the climatological mean. Red contours are isolines at 1.2 °C. **d,** Correlation of SSS recorded by the mooring at the beginning of September with SST from NOAA. Thick contours mark the 95% confidence level and thin contours represent isolines at intervals of 0.2.

Figure 3 | Summer constraints on the hydrographic evolution in the Labrador Sea. a,c,e, Correlation of salinity, temperature and stratification in the Labrador Sea with F_{IS}, where stratification is expressed by means of the vertical potential density gradient. **b,d,f,** Same with F_{LS}. Thick contours delineate the 95% confidence level and thin contours represent isolines at intervals of 0.2. The underlying hydrographic time series have been obtained from the mooring and Argo float observations shown in Supplementary Figure 1.

Figure 4 | Summer constraints on the atmospheric evolution in fall and winter. a,b, Regression of the SLP and surface heat fluxes (HFX, positive downward) from September to mid October onto F_{IS}, obtained from reanalysis data. **c,d,** Same as in **a** and **b** but for the SLP and HFX from November through March. A positive HFX anomaly in winter implies that the ocean is losing less heat. Thick contours delineate the 95% confidence level and thin contours show isolines of the correlation at intervals of 0.1 in **a** and **c** and 0.2 in **b** and **d**.

Figure 5 | Trends in the forcing parameters, 1990–2014. a,c, Spatial distribution of the trends in the SST in August and the heat fluxes (HFX, positive downward) in February. **b,d,** Seasonality of the trends in SST over the Irminger Sea and HFX over the Labrador Sea, with the exact regions being delineated by black contours in **a** and **c**. The red lines in **a** and **c** and the envelopes in **b** and **d** indicate the 95% significance intervals.

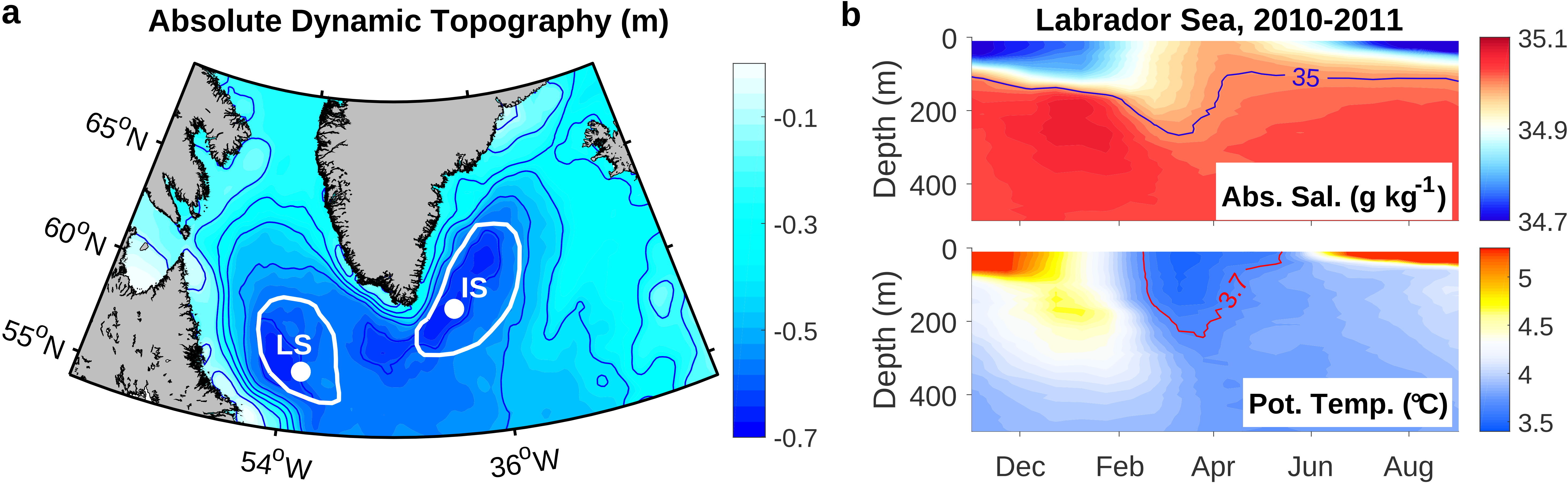

a
Absolute Dynamic Topography (m)
65°N
60°N
55°N
54°W
36°W
LS
IS
-0.1
-0.3
-0.5
-0.7
b
Labrador Sea, 2010-2011
Depth (m)
0
200
400
35
Abs. Sal. (g kg^{-1})
35.1
34.9
34.7
3.7
Pot. Temp. (°C)
5
4.5
4
3.5
Dec
Feb
Apr
Jun
Aug

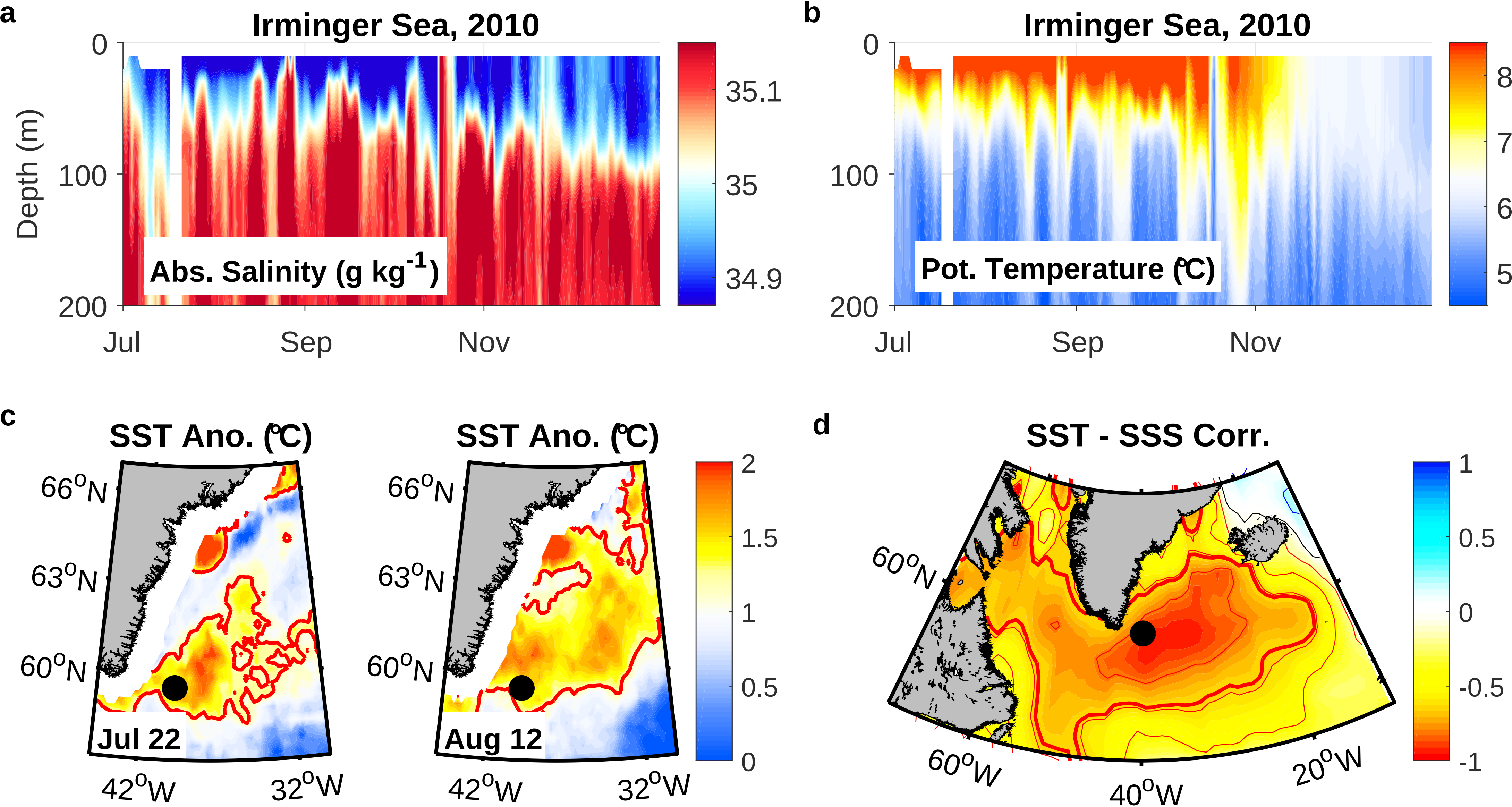

a
Irminger Sea, 2010
Depth (m)
0
100
200
Jul
Sep
Nov
Abs. Salinity (g kg-1)
35.1
35
34.9
b
Irminger Sea, 2010
0
100
200
Jul
Sep
Nov
Pot. Temperature (°C)
8
7
6
5
c
SST Ano. (°C)
66°N
63°N
60°N
Jul 22
42°W
32°W
SST Ano. (°C)
66°N
63°N
60°N
Aug 12
42°W
32°W
2
1.5
1
0.5
0
d
SST - SSS Corr.
60°N
60°W
40°W
20°W
1
0.5
0
-0.5
-1

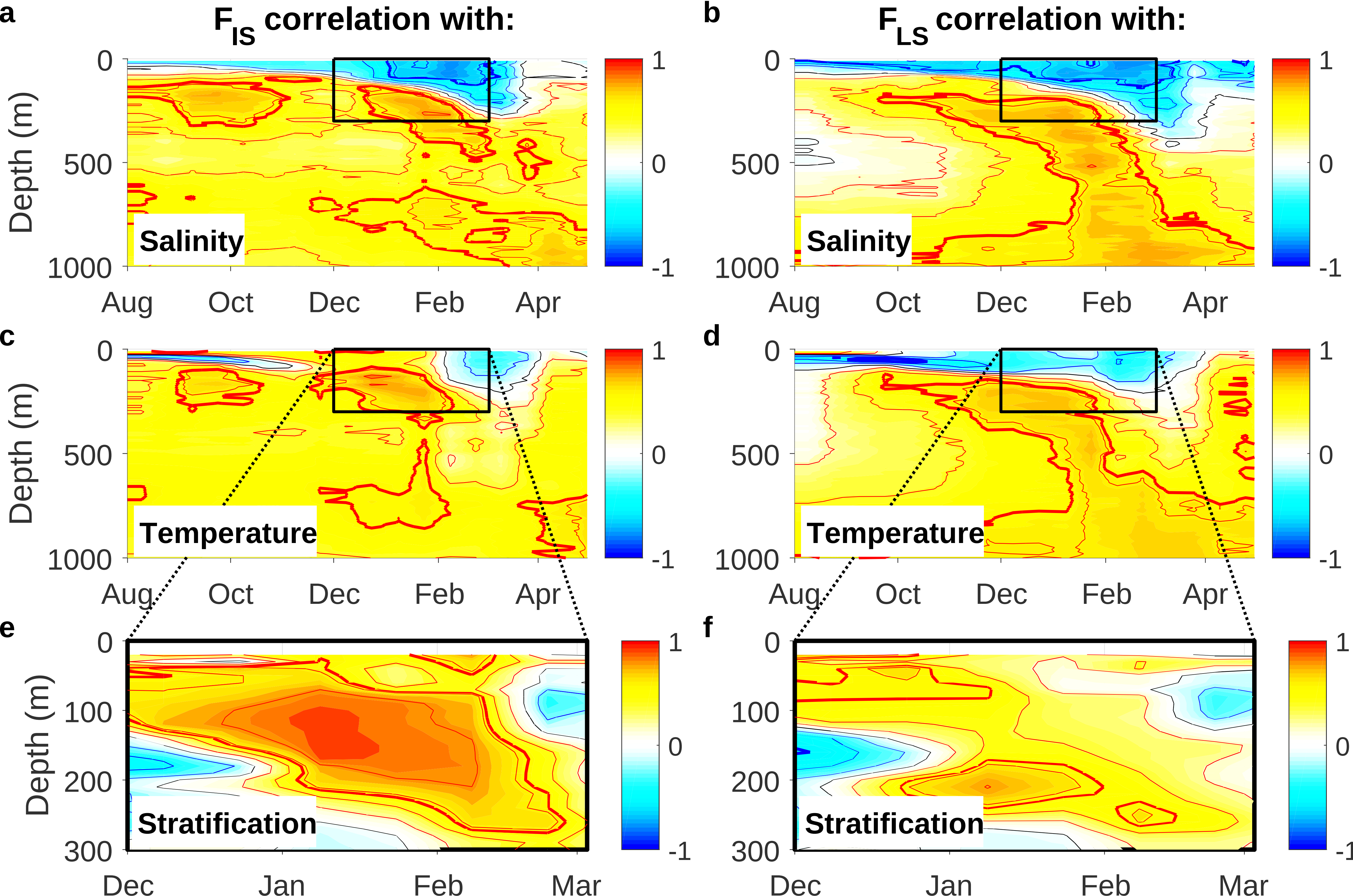

a
F_{IS} correlation with:
b
F_{LS} correlation with:
Salinity
Salinity
c
d
Temperature
Temperature
e
f
Stratification
Stratification
Depth (m)
0
500
1000
100
200
300
Aug
Oct
Dec
Feb
Apr
Jan
Mar
1
0
-1

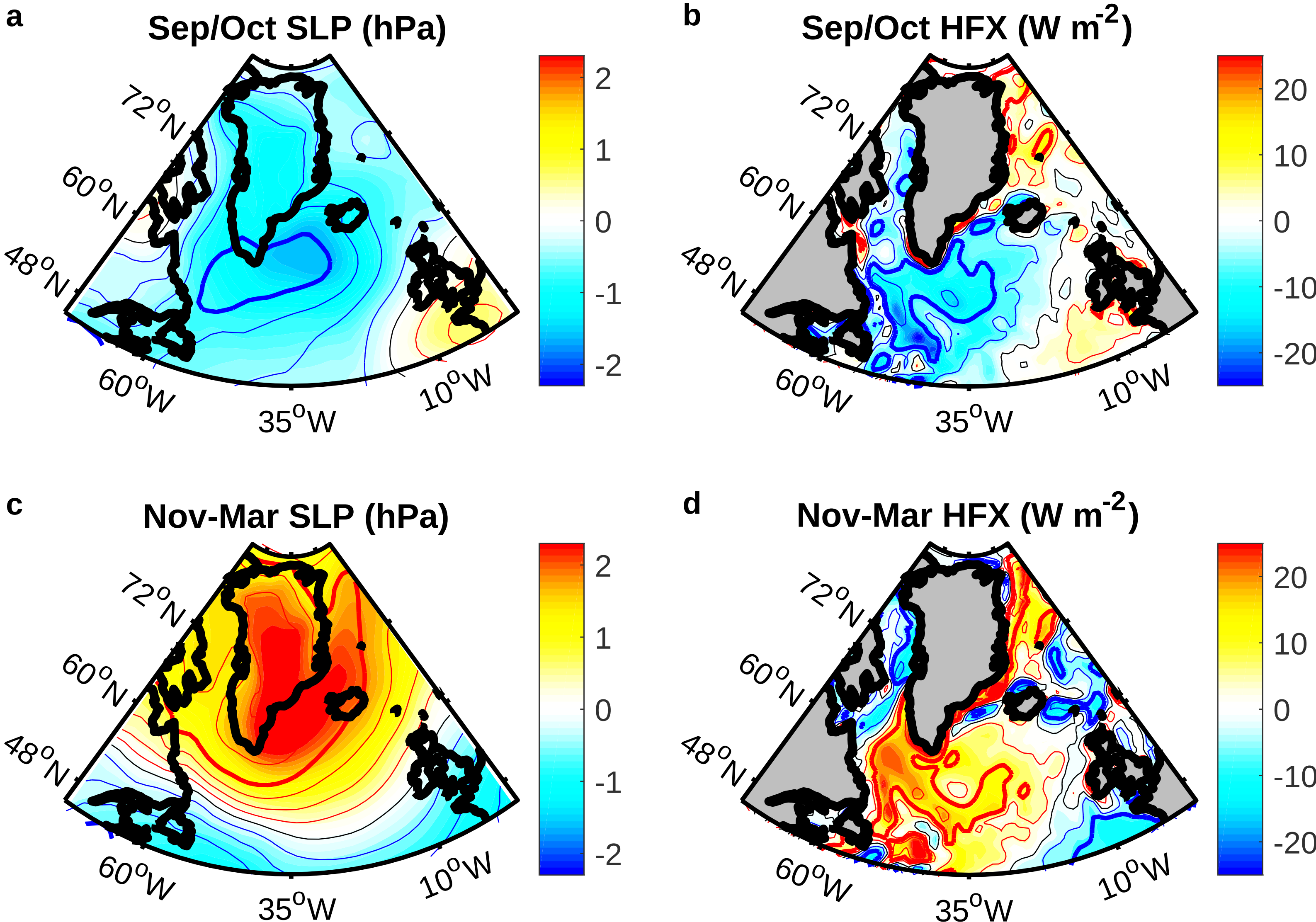

a
Sep/Oct SLP (hPa)
b
Sep/Oct HFX (W m-2)
c
Nov-Mar SLP (hPa)
d
Nov-Mar HFX (W m-2)
72°N
60°N
48°N
60°W
35°W
10°W
2
1
0
-1
-2
20
10
0
-10
-20

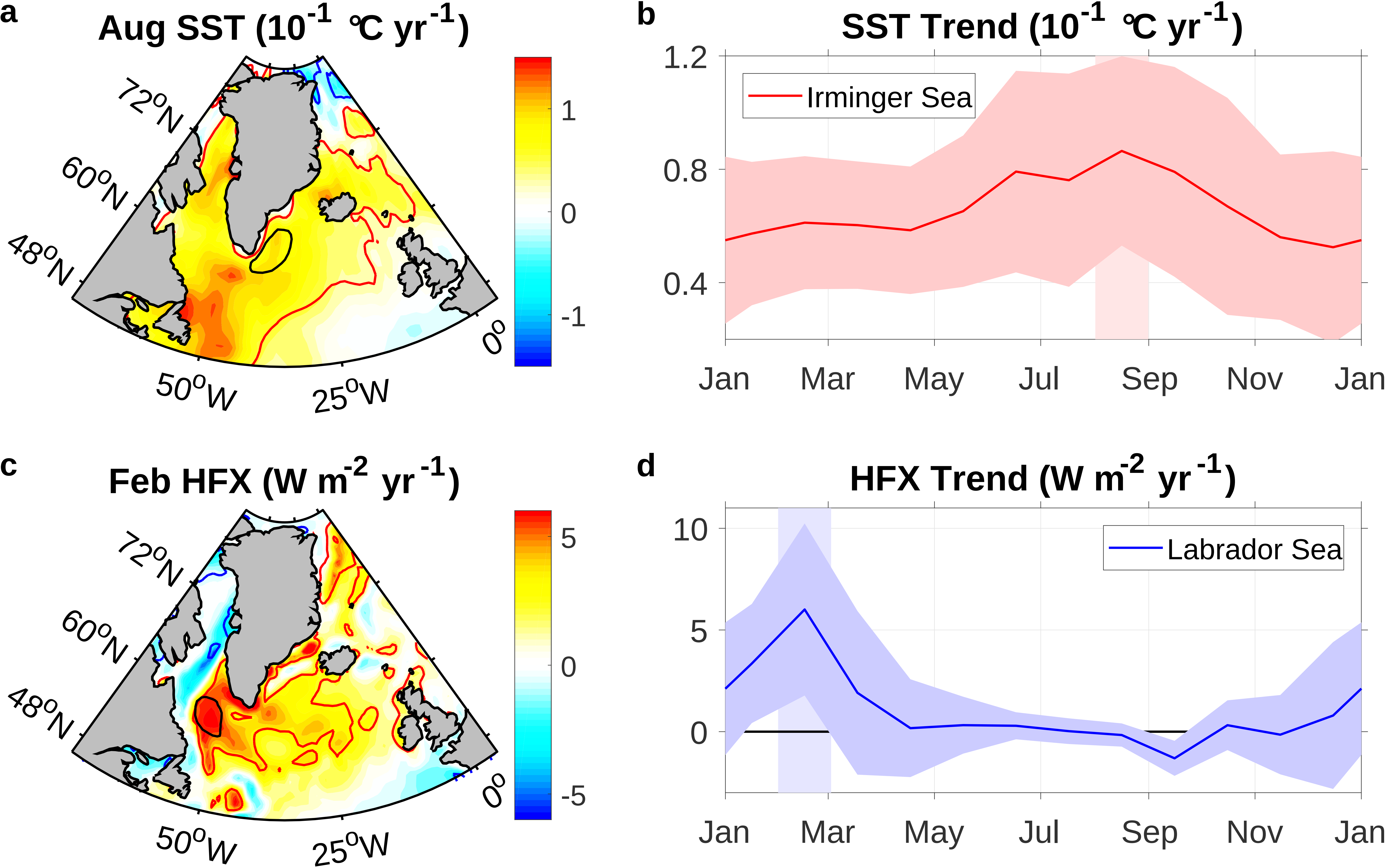

a
Aug SST (10^-1 ℃ yr^-1)
72°N
60°N
48°N
50°W
25°W
0°
1
0
-1
b
SST Trend (10^-1 ℃ yr^-1)
Irminger Sea
1.2
0.8
0.4
Jan
Mar
May
Jul
Sep
Nov
Jan
c
Feb HFX (W m^-2 yr^-1)
72°N
60°N
48°N
50°W
25°W
0°
5
0
-5
d
HFX Trend (W m^-2 yr^-1)
Labrador Sea
10
5
0
Jan
Mar
May
Jul
Sep
Nov
Jan